ACS OMEGA

http://pubs.acs.org/journal/acsodf

Article

Amide Functionalized Mesoporous MOF LOCOM-1 as a Stable Highly Active Basic Catalyst for Knoevenagel Condensation Reaction

Sheereen Afaq, Muhammad Usman Akram, Wasif Mahmood Ahmed Malik, Muhammad Ismail, Abdul Ghafoor, Muhammad Ibrahim, Mehr un Nisa, Muhammad Naeem Ashiq, Francis Verpoort,* and Adeel Hussain Chughtai*

Cite This: *ACS Omega* 2023, 8, 6638−6649

Read Online

ACCESS | Metrics & More | Article Recommendations | Supporting Information

ABSTRACT: Acyl-amide is extensively used as functional group and is a superior contender for the design of MOFs with the guest accessible functional organic sites. A novel acyl-amide-containing tetracarboxylate ligand, bis(3,5-dicarboxy-pheny1)terephthalamide, has been successfully synthesized. The H_4L linker has some fascinating attributes as follows: (i) four carboxylate moieties as the coordination sites confirm affluent coordination approaches to figure a diversity of structure; (ii) two acyl-amide groups as the guest interaction sites can engender guest molecules integrated into the MOF networks through H-bonding interfaces and have a possibility to act as functional organic sites for the condensation reaction. A mesoporous MOF ($[Cu_2(L)(H_2O)_3]\cdot 4DMF\cdot 6H_2O$) has been prepared in order to produce the amide FOS within the MOF, which will work as guest accessible sites. The prepared MOF was characterized by CHN analysis, PXRD, FTIR spectroscopy, and SEM analysis. The MOF showed superior catalytic activity for Knoevenagel condensation. The catalytic system endures a broad variety of the functional groups and presents high to modest yields of aldehydes containing electron withdrawing groups (4-chloro, 4-fluoro, 4-nitro), offering a yield > 98 in less reaction time as compared to aldehydes with electron donationg groups (4-methyl). The amide decorated MOF (LOCOM-1-) as a heterogeneous catalyst can be simply recovered by centrifugation and recycled again without a flagrant loss of its catalytic efficiency.

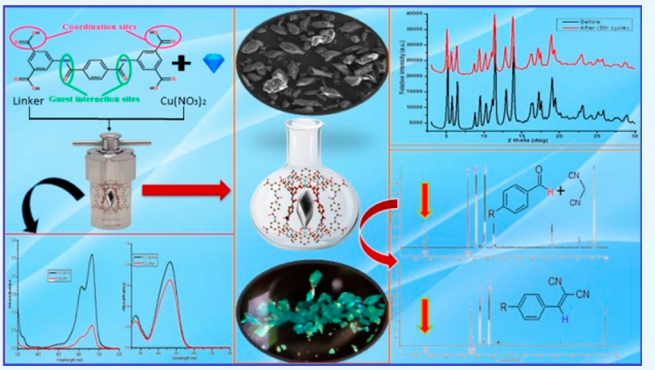

INTRODUCTION

The chemical industry has appeared as a vivacious part of the world economy.[1] Conversely, the manufacture of fine chemicals results in an enormous scale of environmentally injurious waste material. Heterogeneous catalysis is taking on a progressively imperious role in chemical production frequently with an outcome of a crucial drop in waste.[2] For environmental and economic motives, there is an enormous enticement to substitute the homogeneous catalytic systems with effectual and green heterogeneous systems.[3] Heterogeneous catalysis is better than homogeneous catalysis for minimized waste, reusability, clean and green products, and easier separation.[4]

Being a progressive class of the porous materials, metal organic frameworks have elite features of eternal porosity,[5] extreme crystallinity,[6] unrivaled flexibility,[7] unvarying pore sizes,[8] constant and manageable morphologies,[9] exceptional thermal stability,[10] remarkably larger surface areas,[11] and additional edges of lesser density,[12] i.e., 0.13 g cm^{-3}, along with exclusive features of pore size tunability,[13] adaptable host−guest interactivity,[14] enhanced pore dimensionality (98 Å),[15] and functionality.[16]

Over the past few years, considerable efforts have been enamored for designing and building transition-metal-atom-based metal−organic frameworks having multifunctional ligand bridging moieties that tend to impart structure multiplicity as well as fascinating features, for instance, molecular recognition,[17] therapeutics and diagnostics in biomedicine,[18−20] magnetism,[21−23] molecular separation,[24] thin film systems,[25] drug delivery,[26] solar cells,[27] electric conductance,[28] carriers for nanomaterials,[29] oxygen evolution reaction,[30] capture of CO_2,[31] sensing,[32] luminescence,[33] adsorption,[34] renewable energy,[35,36] gas storage,[37,38] separation,[39] proton conduction,[40] heterogeneous catalysis,[41−45] asymmetric heterogeneous catalysis,[46] electrolysis,[47] and drug delivery.[48] Particularly, MOFs have attribute features that include (i) dynamic behaviors in response to the guest molecules, (ii) well-ordered porous

Received: November 4, 2022
Accepted: February 1, 2023
Published: February 10, 2023

https://doi.org/10.1021/acsomega.2c07137
ACS Omega 2023, 8, 6638−6649

structures, and (iii) flexible, designable channel surface functionalities. Various kinds of ligands in copious synthetic approaches have been employed in order to produce some inimitable frameworks. Among those, polypyridine,[49] hybrid ligands,[50] polycyanate,[51] or polycarboxylate,[52] in which a range of spacer groups attach either cyanate or pyridine or carboxylate or a combination of all, are common choices for the building of metal organic networks.

One of utmost divergent fields of MOF investigation is their use as a heterogeneous catalyst. Actually, catalysis using a MOF as a catalyst depends on active catalytic sites within the MOF framework; both metal centers and organic ligands within the framework of MOF constrain to proficient catalytic activities.[53] In past two decades, utilization of MOFs as a heterogeneous catalyst has offered a connotation surge as MOFs have been deliberated upon as an environmentally friendly alternative for heterogeneous catalysis. The separation of reaction target products, fewer leaching problems, and reusability of the catalyst make MOFs dynamic heterogeneous catalysts. The high porosity, multifunctionality, and pore tunability are engaging MOFs at the frontier between enzymes and zeolites. A wide diversity of MOF frameworks have been constructed with diverse linkers as well as numerous transition metals and have been evaluated in the heterogeneous catalysis for a variety of organic reactions, but still numbers of MOF materials are unexplored for catalysis. Hence, practice of the MOFs in catalysis is enormously wide and growing incessantly.

Two kinds of strategies that are presently utilized to functionalize the MOF channels are immobilization of coordinatevely unsaturated or open metal sites (OMSs) and exordium of the functional groups to deliver guest-accessible functional organic sites (FOSs).[54,55] There is emergent curiosity in making use of OMSs for precise gas adsorption and Lewis acid catalysis, but lesser attention has been concerned with the study of the functional organic sites, regardless of their significance. A scarcity of reports on the FOS is due to the intricacy of constructing guest-accessible functional organic sites on the pore exterior: these functionalities tend to coordinate the metal ions, coming out in the frameworks where FOSs are entirely blocked.[56] In contrast to utilizing OMSs to build functionalized MOFs, a study on the addition of the FOSs in the MOFs is lesser reported, which is probably due to the complexity endured in making guest accessible functional organic sites on pore surfaces of MOF because the organic functionalities tend to interrelate with the metal ions that come out in blocking functional organic sites within the MOF frameworks.

Even though MOFs have provided an advanced platform for heterogeneous catalysis and multifold publications regarding MOF catalysis have been recounted, still there is a challenge to establishing their durability, specificity, and catalytic activity under all provided reaction conditions accordingly. Including all categories of heterogeneous catalysts together with MOFs diminishes when used for a prolonged time of activity. Plenty of research is available that primarily addresses the reliability of MOFs, though a minor number of publications emphasize the turnover numbers as well as turnover frequencies and consequently compare them with those of other relevant catalysts. By means of spectroscopic and textural techniques, the catalyst deactivation can be easily tracked.[57] Comparatively lower thermal stability is another determinant that hinders MOF applications for reactions taking place over higher temperatures. Equally, leaching of inorganic metal entities or that of organic linker entities in a reaction medium is a loathsome practice for the heterogeneous catalysis route. Hence, it must be settled throughout the reaction and can be easily spotted either by means of the hot filtration test or by means of chemical analysis based on the reaction filtrate, consequently. Ultimately, there is a prerequisite of analytical review-based research for justifying the catalytic performances of MOFs; additionally their chemical as well as thermal consistency in catalysis must be screened out thoroughly.

By incorporating the fundamental functional groups like pyridyl,[58] amide,[59] and amino,[60] extremely dynamic solid basic heterogeneous MOF catalysts can be achieved. While incorporated basic organic functional groups are an essential part of organic linkers in MOFs, leaching of metal does not happen, resulting in a steady system.

One more predominant functional moiety is acylamide, which possesses both an electron acceptor site (−NH moiety) as well as an electron donor site (−C═O moiety) simultaneously and hence has been ascertained as a strong entrant for the synthesis of MOF edifices enriched with FOSs that are easily accessible by incoming guest molecules.[61] A number of groups have synthesized the functionalized MOF edifices by simply engaging the acylamide moiety as a FOS with the aim to achieve efficient catalysis as well as selective adsorption within the frameworks exclusively. Numerous research groups have productively constructed the functionalized metal organic frameworks by utilizing the amide groups as functional organic sites for the catalysis and/or selective adsorption in MOF networks.[61] The Knoevenagel condensation of aromatic and aliphatic ketones or aldehydes with active methylenes (containing two electron-attracting groups) was reported by Knoevenagel.[62] Knoevenagel's first papers in this field were concerned with condensation of diethyl malonate with ethyl benzoylacetate and formaldehyde.[62]

Knoevenagel condensation is a productive reaction for the formation of C═C bonds having various applications in the synthesis of pharmaceuticals (metallothionein-3 (MT3) ligand, 2-pyrone derivatives) and fine chemicals.[63−65] Knoevenagel condensation is a strategic step in the industrial scale manufacture of antimalarial drug lumifantrine (a constituent of coartem).[66,67] The reaction has a wide range of applications regarding coumarin and its derivatives' synthesis that is a significant moiety of organic compounds and is also employed as additives in both cosmetics and the food industry.[68] Knoevenagel condensation has been employed in the total synthesis of a multitargeted kinase inhibitor.[69] It has various relevances in the production of fine chemicals and heterocyclic as well as carbocyclic compounds of the biological corollary.[63] There is bountiful connotation in the Knoevenagel products as a virtue of their biological activity; for example, the tryphostins (a class of tyrosine phosphorylation inhibitor), such as α-cyano-thiocinnamide, are recognized to inhibit the autophosphorylation of EGFR (epidermal growth factor receptor), in addition to possessing antiproliferative effects on the keratinocytes.[70]

A number of catalysts have been noted for catalyzing this C═C bond forming reaction (Knovengel condensation); for instance, zeolites,[71] organo-catalysts,[72] surfactants,[73] ionic liquids immobilized in the mesoporous silica,[74] or surface alteration in the presence of the alkali metal ions.[75] But from an application viewpoint, a number of these catalysts experience drawbacks such as using carcinogenic and hazardous materials. Furthermore, the Knoevenagel condensation

https://doi.org/10.1021/acsomega.2c07137
ACS Omega 2023, 8, 6638−6649

reaction is commonly catalyzed by acids or bases and necessitates extreme reaction conditions such as high reaction temperatures[76] and microwave irradiation.[77] An acylamide adorned Cu-MOF was reported by Cheng et al.[78] For Knoevenagel condensation, the mentioned MOF presented exceptional catalytic performance. A number of functionalized MOFs having acylamide enriched organic linkers were reported by Kitagawa et al. These functionalized MOFs presented fascinating selective adsorption as well as appealing heterogeneous catalytic performances.[79] Similarly, a Cu(II)-organic framework was reported by Kostakis et al. that possessed a flexible terepthaloyl-bis-glycinate linker that displays a dexterous heterogeneous catalysis for 3,5-di-*tert*-butylcatechol (DTBC) oxidation.[80] The Bai[81,82] and the Sun[83] research groups have produced a sequence of MOFs having acyl-amide-containing carboxylate linkers; all of the prepared MOFs reveal remarkabe CO_2 capture capacity. The research about the acyl-amide adorned MOFs is relatively inadequate due to the intricacy in fabricating the guest accessible acyl-amide entities as guest accessible sites with cavities, as these functional moieties are labile to interrelate with the metal ions. Adorning MOF edifices containing various functional organic sites will enrich functionalized metal organic framework chemistry and will definitely expedite the achievement of enhanced performances of respective MOFs.

We successfully synthesized a new nanosized acylamide decorated tetracarboxylate linker, namely, bis(3,5-dicarboxy-pheny1)terephthalamide (H_4L), presented in Scheme 1. The

Scheme 1. Structure of Linker (Bis(3,5-dicarboxy-pheny1)terephthalamide) Showing Their Potential Connectivity through Carboxylate (Coordination Sites) and Amide Linkage As the Guest Interaction Sites

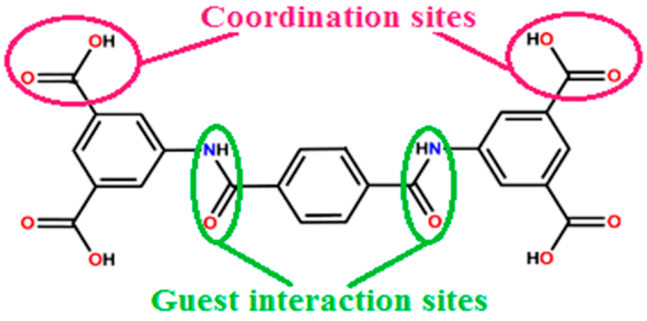

prepared H_4L ligand possesses numerous fascinating attributes as follows: (i) a multiplicity of structures because of rich coordination patterns developed by four carboxylate moieties that serve equally as coordination sites and (ii) two acyl-amide assemblies as the guest accessible sites that can encourage guest molecules assimilated into the MOF framework through H-bonding interactions and contain the ability to function as a guest interaction FOS. Herein, we report the synthesis and characterization of $[Cu_2(L)(H_2O)_3]S_x{\cdot}n$ (S, solvent molecule: water or DMF molecule, and x is the number of S). Moreover, catalytic properties of prepared MOFs in the Knoevenagel condensation of diverse aldehydes (benzaldehyde, *p*-substituted benzaldehydes) with the active methylene compound (malononitrile) were explored. The catalysis results illustrated that the MOF exhibits good activity in the base-catalyzed Knoevenagel condensation of aromatic aldehydes exclusive of a considerable loss of activity.

RESULT AND DISCUSSION

Numerous metal organic frameworks have been built with the amide adoring manifold carboxylate linkers. In the recent past, Zou et al. have reported an iso-structural MOF with cobalt, synthesized from bis(3,5-dicarboxy-pheny1)terephthalamide with lon topology 4-linked CO_2 groups and the nanosized tetra-carboxylate linker.[84] We also designed and synthesized Cu-MOF (LOCOM-1) from an amide-containing tetra-carboxylate ligand (bis(3,5-dicarboxyphenyl)-tere-phthala-mide) containing paddle wheel SBUs $[Cu_2(COO)_4]$ (secon-dary building units) using a mixed solvent DMF/H_2O (ratio 3:1) solvothermal process.[85]

The acylamide groups in the linker increases the arms of the linker, which can possibly produce a large internal cavity in the Cu-MOF and moreover increases the flexibility of the linker, which would facilitate making both boat and chair con-formations in the lon network. The blue block crystals of $[Cu_2(L)(H_2O)_3]{\cdot}4DMF{\cdot}6H_2O$ were obtained solvothermally by reacting H_4L and $Cu(NO_3)_23H_2O$ in the presence of a binary solvent (having composition 60% dimethylformamide (DMF) along with 20% water) at 85 °C for 3 days.

The PXRD analysis of LOCOM-1 is shown in Figure 1a. The PXRD results demonstrate that the experimental PXRD patterns have intense peaks, evidencing a good, pure phase of the crystal. The TGA curve disclosed a 25% weight loss in a temperature range of 20−280 °C, which corresponds to four DMF and nine water guest molecules eliminated (overall calculated weight loss is 24.78%). The TGA record for Cu-MOF is emblematic of the two steps of weight loss for guest molecules: four DMF molecules and nine H_2O molecules per formula unit. Hence, TGA analysis of the prepared MOF pointed out that prepared material was thermally stable up to a temperature range of 300 °C; beyond this range, prepared Cu-MOF gradually decomposes and ends at above 510 °C (Figure 1b).

The microscope image of LOCOM-1 shows bright bluish shaped rhombohedron shaped crystals (Figure S5). Figure 2 illustrated the SEM images of the Cu-MOF obtained from the ligand (H_4L) along with metal salt, namely, $Cu(NO_3)_2{\cdot}3H_2O$ inside a binary mixed solvent, i.e., DMF/H_2O, having single drop of 2 M HCl as well. The SEM micrograph revealed the attainment of a precise block of bluish crystalline material as was anticipated. Some rhombohedra with distinct facets can be recognized (Figure 2a,b).

FTIR spectra of Cu-MOF and H_4L are shown in Figure 3. The FTIR pattern of the mesoporous Cu-MOF divulged the existence of the two significant bands at 1587 and 1370 cm^{-1} that designate vibrations of the carboxylate symmetric stretching (υ-COO^- 1400−1310 cm^{-1}) and antisymmetric stretching (υ-COO^- 1630−1500 cm^{-1}), which were lower than the stretching vibration of carbonyl of the carboxylic acid group (υ C═O, 1760−1690 cm^{-1}) professed for the free carboxylic groups in H_4L (Figure 3). The two mentioned bands were associated with the carboxylate ion ($-COO^-$) vibrations that confirm the existence of the carboxylate ions in the Cu-MOF framework. The resilient absorption band of the carbonyl group in H_4L at 1711 cm^{-1} disappeared in Cu-MOF, indicating that full deprotonation of the carboxylic acid moieties in the Cu-MOF proves the change of the carboxyl moieties into the carboxylate ones and moreover acclaims that the H_4L ligand becomes coordinated with Cu(II) when the reaction is accomplished. The coordination of the Cu ions with

https://doi.org/10.1021/acsomega.2c07137
ACS Omega 2023, 8, 6638−6649

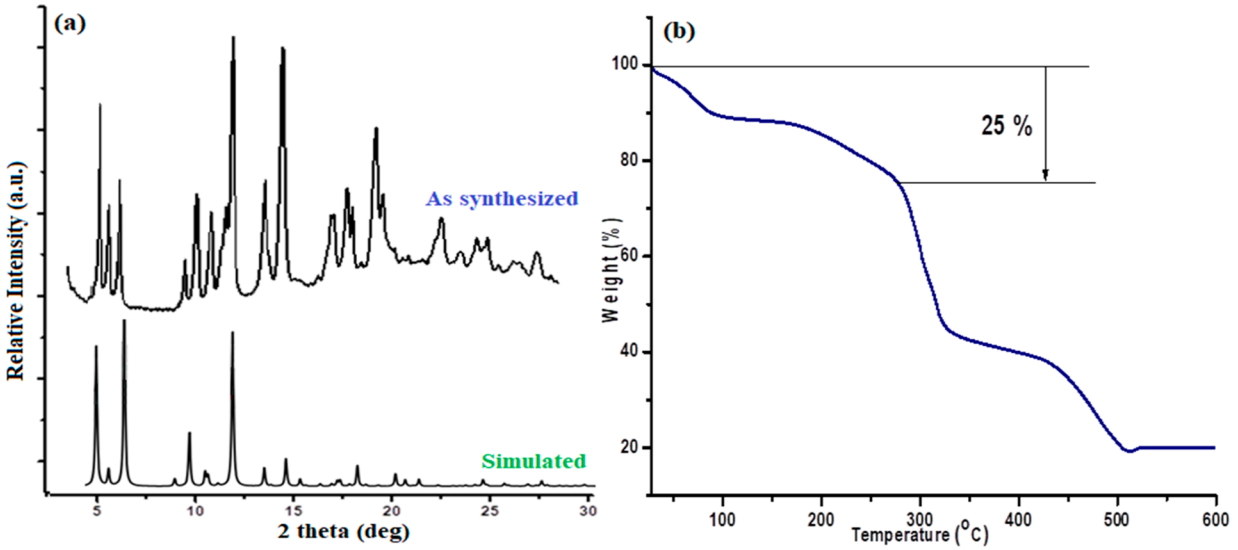

Figure 1. PXRD (a) and TGA (b) of Cu-MOF.

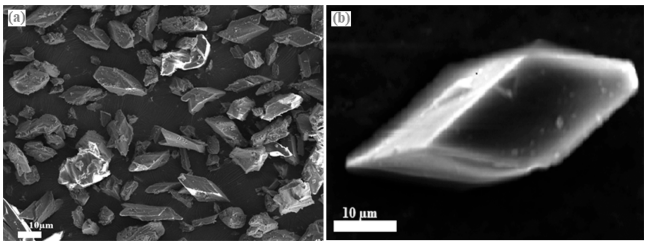

Figure 2. (a) SEM image of Cu-MOF (10 μm) representing crystals of Cu-MOF and (b) single rhomohedral crystal of Cu-MOF.

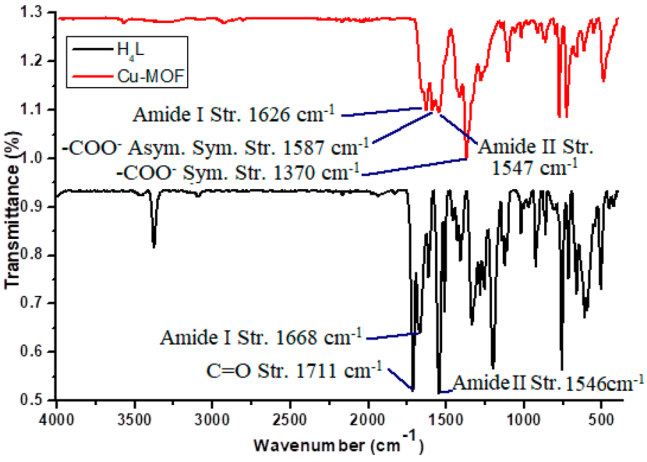

Figure 3. FTIR spectrum of H_4L and Cu-MOF.

the provided ligand, namely, H_4L, ensues in the efficacious synthesis of Cu-MOF. An apparent band for N−H was perceived at 3554 cm^{-1} that was indicative of the presence of amide N−H coordinated with water in the MOF. The amide I band appearing at 1668 cm^{-1} in the ligand shifted down to 1626 cm^{-1} in MOF. The bands lower than 900 cm^{-1} fit in for different C−H bond bending vibrations that usually tend to lie in the 900−800 cm^{-1} range, whereas C═C−H aromatic ring deformation bands usually lie in the 780−670 cm^{-1} range. For H_4L, a peak at 1333 cm^{-1} was observed that points out the presence of C−N stretching vibrations. Later, this mentioned peak value in prepared MOF spectra was dropped to 1276 cm^{-1}.

Permanent porosity of mesoporous $[Cu_2(L)(H_2O)_3]\cdot 4DMF\cdot 6H_2O$ is checked by their N_2 sorption isotherm at 77 K. First, the Cu-MOF was soaked in CH_3OH for 3 days and then in CH_2Cl_2 for 3 days also and finally evacuated at room temperature after about 2 h to get the actuated Cu-MOF prior to BET analysis. The N_2 adsorption−desorption isotherm of Cu-MOF demonstrates the typical type-IV curve, that is, illustrating pore compression with distinct sorption hysteresis (Figure 4a). The N_2 sorption isotherm results describe the existence of mesopores with 352 cm^3/g of N_2 uptake for Cu-MOF (64.725 m^2/g of BET surface area and 71.15 m^2/g of Langmuir surface area). The pore diameter (width) and pore volume observed were 26.65 nm and 0.43 cm^3/g, respectively. The CO_2 and CH_4 sorptions were also performed at STP to probe the uptake of CO_2 and CH_4 in MOFs (Figure 4c and b). The sorption study of both gases proves that MOFs possess a maximum CO_2 and CH_4 of 13.87 and 4.54 cm^3/g, respectively. The higher adsorption value of CO_2 is primarily because of the small molecular size of CO_2 in contrast to CH_4.

Because the prepared MOF is not only of interest for gases, in order to further explore the permanent porosity of prepared MOFs, organic dye adsorptions in water were investigated. Two different kinds of dyes, methyl orange (MO) and methyl blue (MB), were chosen as models for the experiments. A total of 10 mg of MOF was poured into 10 mL of an aqueous organic dye solution of 100 $mg\cdot L^{-1}$ at room temperature under stirring. The magnetic stirring of prepared dye solutions having an adsorbent was carried out and was upheld for a fixed time frame (12 h) at 25 °C and kept in the dark to ensure the establishment of an adsorption−desorption equilibrium. After centrifugation, with the help of UV−vis spectroscopy, the plasma was evaluated, or after dilution (if necessary). For the $[Cu_2(L)(H_2O)_3]\cdot 4DMF\cdot 6H_2O$ (Cu-MOF), the dye adsorption percentages studied were 88.59% for MB and 21.19% for MO (Figure 5). The difference in adsorption rates could be attributed to the different molecular sizes of used dyes. However, the percentage adsorption for MB dye was comparatively higher than that of MO percentage adsorption. A possible reason for the higher percentage of MB could be

https://doi.org/10.1021/acsomega.2c07137
ACS Omega 2023, 8, 6638−6649

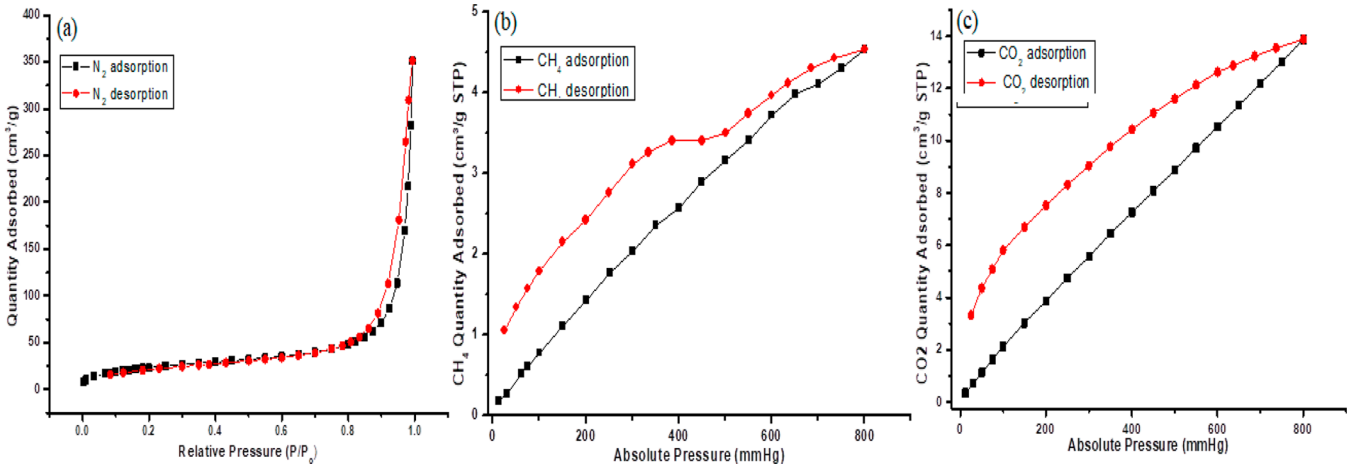

Figure 4. (a) Nitrogen sorption isotherm, (b) CH_4 sorption isotherm, and (c) CO_2 sorption isotherm.

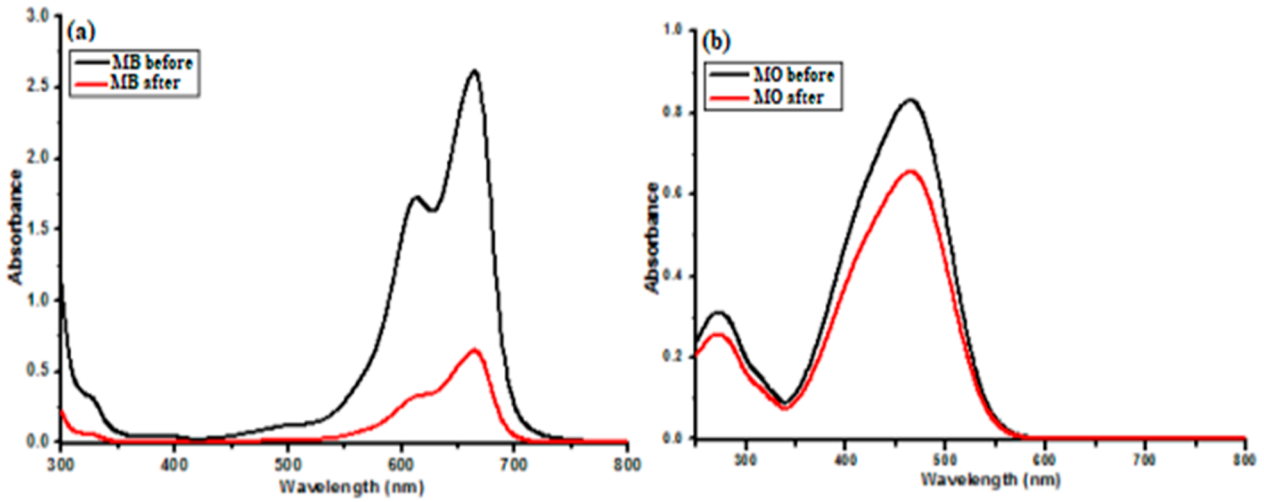

Figure 5. UV−vis spectra of aqueous solutions of dyes with Cu-MOF: (a) MB, (b) MO.

related to its smaller molecular size, while the size of methyl orange was comparatively larger so molecules of MB dye can easily penetrate inside pores of the prepared MOF and hence can comparatively elevate its adsorption rate accordingly.

KNOEVENAGEL CONDENSATION

Knoevenagel condensation is a broadly used reaction in the industry and research and is of great significance for numerous pharmaceutical products. Normally, organo-bases catalyze the mentioned renowned reaction, i.e., pyridine-based basic catalysts or piperidine-based basic catalysts. On the other hand, these homogeneous base catalysts seem to follow lengthy tedious reaction routes. Furthermore, they end up in undesirable side reactions. For instance, oligomerizations may result, requiring high temperatures for accomplishment, and recovering the used catalyst is also not an easy job. Numerous reports on the heterogeneous Knoevenagel catalysts, for example, magnetic base analogues or ionic liquids, modified zeolites, have been reported, leading to cleaner products while the complex neutralization processes can be skirted. Furthermore, these catalysts can be regenerated and recovered. Knoevenagel condensation of various aromatic, aliphatic, and heterocyclic aldehydes with malononitrile substrates using different catalysts first entails the heating of the reaction mixture and second requires comparably more time for reaction completion. Without exploiting any catalyst, the Knoevenagel condensation of various benzaldehydes involving active methylene substrates could not be accomplished.

All reactions were performed with different *p*-substituted benzaldehydes and malonitriles in DMSO-d_6 using LOCOM-1 without using any organic or inorganic base. ^{1}HNMR spectroscopy was used to observe the progress of the reaction and to conclude reaction yield. It took a time period of just 3−6.5 h for analyzing all reactions involving alkene derivative synthesis with an excellent productivity of 95−99% yield as well. The first step is the formation of a carbanion from malononitrile via basic Cu-MOF. The carbanion attacks the electron-deficient carbon (partially positive) of the benzaldehyde substrate, while the carbonyl oxygen (partially negative) present in benzaldehyde takes back the exact same proton that was taken out during enolate formation. The hydrogen from α-carbon was removed by a lone pair present on the newly formed hydroxyl group. Finally, the double bond (propanedinitrile-2-[(phenyl) methylene) formation is accomplished by involvement of a lone pair donated by α-carbon; meanwhile, elimination of a water molecule also occurs. As illustrated in Table 1, reaction of benzaldehyde gave the final product in 98% yield with 2451 TONs (Table 1, entry 1). High yields from 95 to 100% were attained for various benzaldehydes

https://doi.org/10.1021/acsomega.2c07137
ACS Omega 2023, 8, 6638−6649

Table 1. Knoevenagel Condensation Reactions of Different Benzaldehydes with Malononitrile over Cu-MOF[a]

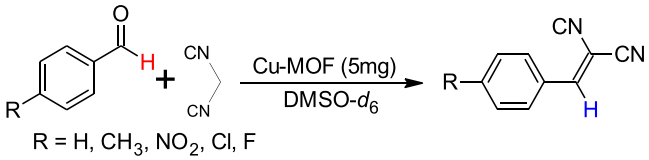

R = H, CH_3, NO_2, Cl, F

entry	R	time (minutes)	yield[b] (100%)	TON[C]
1	H	390	98.05	2451
2	CH_3	435	95.63	2390
3	F	180	99.92	2498
4	Cl	260	100	25000
5	NO_2	20	99.4	2485

[a]Reaction conditions: All reactions were performed with 1 mmol of benzaldehyde and 1.1 mmol of malononitrile in 4 mL of DMSO-d_6 using 0.005 g (0.04 mmol based on amide in MOF). [b]Determined by ^{1}H NMR, based on starting materials. [C]Turnover number (TON): conversion of benzaldehyde (mol)/catalyst (mol) used.

containing different functionalities at the *p* position, including electron donating and attracting groups (4-NO_2, 4-Cl, 4-F, 4-Me). Impressively, 4- fluorobenzaldehyde and 4-chlorobenzaldehyde revealed reasonable reaction yields of 99 and 100%, respectively. It has been observed that reaction times were interrelated with the electronic effects on the benzaldehydes. Consequently, more reaction times are provided for electron-donating moieties in comparison to respective acceptor ones.

In the case of benzaldehyde (1.0 mmol) and malononitrile (1.1 mmol) as substrates using 5 mg of catalyst, a 98% conversion was achieved. The conversion with time was monitored by ^{1}H NMR. At different time intervals following the time frame sequence, samples were collected and then immediately were subjected to analysis for ^{1}H NMR study. The conversions (yields) were computed by integration of the benzylic protons in each case (Table 2). The conversions of

Table 2. ^{1}H NMR Integration of the Characteristic Benzylic Protons (Starting, Product) and Conversions into Propanedinitrile-2-[(phenyl)methylene]

S. no	time (minutes)	integration starting	integration product	conversion (%)
1	0	1	0.00	0.00
2	5	1	0.03	2.96
3	15	1	0.05	4.76
4	30	1	0.06	5.66
5	90	1	0.15	13.04
6	210	1	0.61	37.88
7	260	1	2.27	69.41
8	330	1	6.07	85.85
9	390	1	64.66	98.05

benzaldehye into propanedinitrile-2-[(phenyl)methylene] calculated were 2.91, 4.76, 5.66, 13.04, 37.88, 69.41, 85.05, and 98.05 at time intervals of 0, 5, 15, 30, 90, 210, 260, 330, and 390 min, respectively (Figure S7).

The Knoevenagel condensation of *p*-methylbenzaldehyde with malononitrile offered 85.6% yield in 435 min (Table S1). The high reaction time of *p*-methylbenzaldehyde is due to a strong + I effect (inductive effect) of the methyl group at the para position. The carbonyl group in benzaldehyde is more electrophilic than the carbonyl group in *p*-methylbenzaldehyde. The more electrophilic the carbonyl carbon of benzaldehyde, the more reactive it is toward the malononitrile. Table S1 shows the conversion of *p*-methylbenzaldehyde into the propanedinitrile-2-[(4-methyl phenyl)methylene] with different time intervals. The progress of the reaction monitored by ^{1}H NMR and spectra of the condensation reaction are provided in the Supporting Information (Figure S8).

Furthermore, aromatic aldehydes having electron withdrawing substitution (4-nitro, 4-chloro, 4-fluoro benzaldehyde) offer yields > 98 in less reaction time as compared to benzaldehaydes having an electron donationg group (Figures S9−S11). Electronic inductive and mesomeric effects can be used to explicate divergent reactivities among different benzaldehydes. Both fluorine and chlorine groups have an electron withdrawing effect on neighboring carbon, accomplishing it electron deficiently. This in sequence has a substantial inductive effect (I) on the aldehydic carbonyl carbon atom. As in the case of fluoro and chlorobenzaldehydes, 99% conversion is achieved within 180 and 260 min, respectively (Tables S2, S3). The conversion of *p*-fluorobenzaldehyde and *p*-chlorobenzaldehyde into propanedinitrile-2-[(4-fluorophenyl)methylene] and propanedinitrile-2-[(4chlorophenyl)methylene] with a time interval is given in Tables S2 and S3, respectively. The high yield of propanedinitrile-2-[(4-fluorophenyl)methylene] in contrast to propanedinitrile-2-[(4chloro phenyl)methylene] is due to the high electron withdrawing effect of fluoro as compared to chloro.

Knoevenagel condensation of 4-nitrobenzaldehyde with malononitrile gave 98% conversion within 5 min (Table S4). The high reactivity of nitrobenzaldehyde can be attributed to the strong negative resonance effect of the nitro group at the para position. The observed order of reactivity of electron withdrawing benzaldehyes was $-NO_2$ > −F > −Cl. The nitro group, for instance, is characteristic of −I and −M effects, while halogen groups have a −I and +M effect. The −I effect of the halogen group is more dominant than its +M effect. The nitro group has improving −I and −M effects, both. That is why *p*-nitrobenzaldehyde gives a Knoevenagel condensation product in less reaction time as compared to *p*-fluoro and *p*-chlorobenzaldehye.

Though a lot of studies have been conducted that discuss MOF networks having acid properties,[4,86−89] only a few reports of the PCPs having base properties are found in the literature.[90−92] To typify the basic properties of Cu-MOF, the Knoevenagel condensations catalyzed by Cu-MOF done at two sites (−NH, −C═O) are simultaneously present inside amide moieties in Cu-MOF and differ from each other with respect to their functions. In Cu-MOF, the −NH (amino group) moiety acts as a hydrogen donor, whereas carbonyl carbon (−C═O) acts as an electron donor. A recent study described the MOFs with a basic carbonyl oxygen atom acting as catalytic interface sites on the channel wall.[91] So, for our prepared Cu-MOF edifice, we also anticipated that the −C═O moiety (base sites) offers guest interaction sites accordingly. A plausible mechanism can be inferred for the Knoevenagel reaction over amide moieties acting as FOSs in our prepared amide functionalized Cu-MOF in Scheme 2.

According to the proposed mechanism, activation of the methylene carbon of malononitrile ensues due to the basic site (−C═O moiety) of the amide group (step 1; Scheme 2). At the same time (step 2), removal of the acidic proton of the methylene carbon of the malononitrile and given to the carbonium anion happens at the basic site of prepared Cu-

https://doi.org/10.1021/acsomega.2c07137
ACS Omega 2023, 8, 6638−6649

Scheme 2. Proposed Mechanism for Knoevenagel Reaction of the Benzaldehyde with Malononitrile in Prepared Cu-MOF

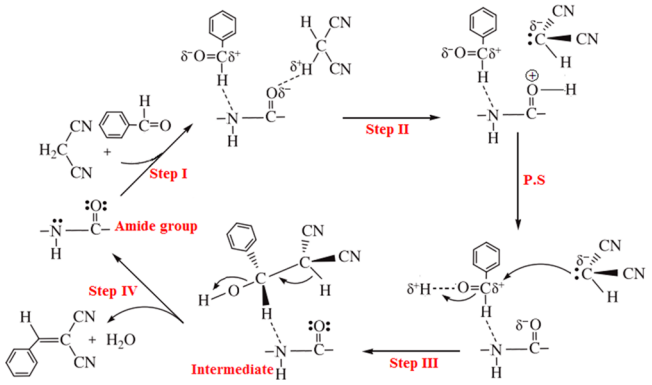

MOF (−C═O). Next is the proton shift (P.S) from the carbonyl oxygen atom of the amide to the carbonyl oxygen atom of the benzaldehyde to make the carbon atom of the benzyl group more electrophilic in nature in order to facilitate the attack for the carbonium ion and removal of water. After the proton shift, the carbonion attacks the electrophilic site of benzaldehyde, namely, the carbonyl moiety, which results in intermediate generation (step 3), which undergoes suitable rearrangement for making dehydration possible (step 4) and eventually leads to final product synthesis. According to the above mechanism, the strength of basicity of the oxygen ion is very imperative for activation of the reactants and subsequent rearrangement of the intermediate inside pores of MOF.

Finally, reusability and recovery of Cu-MOF were conducted. When the condensation reaction between aromatic aldehyde and malononitrile was accomplished, the prepared catalyst (Cu-MOF) was recovered from the reaction mixture by filtration; after that, the catalyst was thoroughly washed away by using ethanol (3 × 10 mL) for complete removal of any obnoxious residue that had adhered onto the catalyst. Subsequently, recovered Cu-MOF (LOCOM-1) catalyst was used again in the next catalytic cycle without any extra treatments.

Recovered catalyst efficiency was assessed again using the same model reaction. Notably, over 97% conversion of the benzaldehyde was retained even after five recycles. As shown in Table 3, a reaction yield of 97% was achieved after five cycles, suggesting that there is no significant loss of activity of the catalyst in process. The results divulged that Cu-MOF maintains easy recovery without losing evident activity. A consistency for PXRD patterns for both fifth-recycled Cu-MOF and a fresh run catalyst was observed that signified an exceptional chemical constancy possessed by the prepared catalyst (Figure S6). The PXRD patterns of the Cu-MOF corroborate that the skeleton of the catalyst remained intact after five recycles.

Table 3. Investigation into the Reuse of Cu-MOF[a]

entry[a]	run[b]	time (minutes)	yield[c] (%)
1.	1	390	98
2.	2	390	98
3.	3	390	98
4.	4	390	97
5.	5	390	97

[a]After each run, the catalyst (Cu-MOF) was isolated by filtration, washed with the ethanol, and dried for the next cycle. [b]Reaction conditions: All reactions were performed with 1 mmol of benzaldehyde and 1.1 mmol of malononitrile in 4 mL of DMSO-d_6 using 0.005 g (0.04 mmol based on amide in MOF) of the as-synthesized Cu-MOF for 390 min. [c]Determined by ^{1}HNMR, based on starting materials.

The effectiveness of Cu-MOF in comparison with numerous catalysts for Knoevenagel condensation within our study is given in Table 4. The obtained TON is better than that of the reported ones. Moreover, in the present work, we did the reaction at room temperature to achieve 98% conversion with 2462 TONs with benzaldehyde and malononitrile. Table 4 represents the Knoevenagel reaction studied with a higher temperature, longer reaction time, and large catalyst loading (amount). In evaluation with other reported catalysts, our Cu-MOF has benefits of being highly active, easy to prepare, and rather cheap and is easily recyclable without a perceptible loss of catalytic activity even after five recycles.

CONCLUSIONS

In summary, we have successfully synthesized a mesoporous Cu-MOF by using an acylamide-containing tetracarboxylate ligand in order to generate the amide FOS within the MOF, which will work as a guest accessible site. The typical illustrious base-catalyzed reaction, namely, the Knoevenagel condensation reaction, was selectively endorsed with excellent yields. The electronic effects of different groups have an impact on the reaction times, with electron donating groups increasing this time obdurately compared to the electron attracting groups. Cu-MOF displays a unique recoverable framework; the mesoporous Cu-MOF can be easily recovered and revealed similar catalytic activity to the initial one even after five cycles. The presented study is predominantly applicable regarding the perspective of the porous solid-state chemistry for the creation of innovative materials having remarkable characteristics resulting from flexible ligand involvement. This result recommended that coordination of transition metal ions and the designed amide functionalized organic linker can give a functionalized MOF with functional organic sites elucidating the base catalytic performance. MOF functionalized with the FOS heralds the next advance in the field of porous materials that can be utilized as a novel enthralling class of heterogeneous catalysts and adsorbents.

EXPERIMENTAL SECTION

Materials. All consumed chemicals were procured from Sigma-Aldrich and well-reputed international and local suppliers. All chemicals were used mainly as such, but when required they were purified via typical techniques, i.e., distillation and recrystallization.

Synthesis. *Synthesis of H_4L.* Synthesis of the amide-containing tertra-carboxylate linker (H_4L, bis(3,5-dicarboxy-pheny1)terephthalamide) was done using a modified version of a previously reported procedure.[103] 5-Aminoisophthalic acid (7.5 mmol, 1.358 g) was added to 10 mL of anhydrous tetrahydrofuran under N_2. Terephthaloyl chloride (3.75 mmol, 0.6713 g) was dissolved with 10 mL of anhydrous THF and was added to the above solution dropwise at a 0−5 °C temperature. After complete addition, the temperature of the reaction was increased to room temperature. Continuous stirring of the mixture was done for a time frame of 24 h, and

https://doi.org/10.1021/acsomega.2c07137
ACS Omega 2023, 8, 6638−6649

Table 4. A Divergence of Catalytic Activity of Numerous MOFs in the Knoevenagel Reaction of Malononitrile and Benzaldehyde

entry	benzaldehyde (mmol)	malononitrile (mmol)	catalyst	quantity	temp	time	yield (%)	TON	ref
1	10	20	JNU-402-NH_2 c	0.06 mmol	80 °C	1 h	99	1665	93
2.	2.1	2	Cd-MOF	0.08 mmol	r.t	12 h	98	1225	94
3	2	2	fiber catalyst $PAN_{EP}F$	0.04 mmol	78 °C	4 h	98	2450	95
4	10	10	$ZnCl_2$	1.0 mmol	100 °C	10 min	90.9	90.9	96
5	10	10	sodium benzoate	0.1 mmol		10 min	98.7	987	97
6	10	10	$LaCl_3{\cdot}7H_2O$	1.0 mmol	85 °C	1 h	95	95	98
7	0.5	0.5	ZnO-3	2.0 mol %	r.t	15 min	92	46	99
8	1.0	1.1	$[Cd(DDIH)_2H_2O]_n$	3.0 mol %	r.t	15 min	96	32	100
9	1.0	1.1	$(Zn(ADA)(L)]{\cdot}2H_2O)_n$	1.0 mol %	r.t	1 h	99	99	101
10	10	20	NUC-54a	0.30 mol %	60 °C	5 h	98	327	102
11	1	1	Cu-MOF (LOCOM-1)	0.04 mmol	r.t	6 h	98	2462	this work

finally white solid was produced. The solid was later filtered as well as washed using THF. Finally, the product was added to a 100 mL beaker, and 30 mL of MeOH was added. The mixture was heated to dissolve excess 5-aminoisophthalic acid. The white solid was subjected to filtration and was thoroughly washed with 10 mL of EtOH (hot) and finally dried in a vacuum. The ^{1}H NMR, ^{13}C NMR, and FTIR spectras of the amide ligand are provided in the Supporting Information (Figures S1−S3). Yield = 3.20 g, 86%. Data for H_4L, selected IR (Solid, cm^{-1}): 3466, 3376, 3094, 1711, 1679, 1666, 1612, 1543, 1510, 1407, 1333, 1281, 1253, 1196, 1122, 9258, 860, 756, 663, 611, 593, 506. ^{13}C NMR (DMSO-d_6, δ ppm): 166.98 (COOH), 166.55 (CONH), 140.13 (C-NH_2), 137.61 (C−C═O), 132.25 (C−COOH), 128.38 (C−H aromatic), 125.26. ^{1}H NMR (DMSO-d_6, δ ppm): 8.17 (4H, ArH), 8.25 (2H, ArH), 8.70 (4H, ArH), 10.75 (2H, CONH), 13.32 (4H, COOH).

Synthesis of $[Cu_2(L)(H_2O)_3]{\cdot}4DMF{\cdot}6H_2O$ or Cu-MOF (LOCOM-1). A 10 mL Teflon vial was acquired in which 4 mL of solvent mixture (DMF/H_2O 3:1 in v/v) was added, and then the prepared ligand (H_4L; 0.05 mmol, 24 mg) was added with a drop of 2 M HCl. To this solution, metal salt $Cu(NO_3)_2{\cdot}3H_2O$ (0.15 mmol, 36 mg) was added in a Teflon vial, and the whole mixture was stirred to homogenize the prepared mixture. Then, the Teflon vial was closed and transferred to the inner steel jacket of an autoclave and heated for 72 h at 85 °C. The targeted Cu-MOF was achieved in the form of blue crystals (Figure S5). DMF washing of the prepared crystals was carried out and crystals were finally dried in the open air. Yield: 42 mg, 64%. $[Cu_2(L)(H_2O)_3]{\cdot}4DMF{\cdot}6H_2O$ ($Cu_2C_{36}H_{58}N_6O_{36}N_6$) Anal. Calcd: C = 40.38%; H = 5.42%; N = 7.85%. Found: C = 41.85%; H = 4.56%; N = 7.23%.

Knoevenagel Condensation. In an model batch experiment, 5 mg of Cu-MOF (the basic catalyst) corresponding to 0.04 mmol of amide groups (based on the total amount of amide groups in Cu-MOF) was added into a solution of 1.1 mmol malononitrile in 4 mL of DMSO-d_6 (solvent) in an Erlenmeyer flask. Finally, the addition of a simple benzaldehyde or *p*-substituted benzaldehyde (1 mmol) into the reaction mixture was done with continuous stirring at room temperature (Table 1). The ^{1}HNMR analysis tool was employed to monitor the reaction progress periodically.

Physical Measurements. NMR (nuclear magnetic resonance) data (^{13}C and ^{1}H) were assembled on a Bruker DPX 500 MHz apparatus in DMSO-d_6 solution, and the chemical shifts were accounted to the internal standard TMS (0 ppm). FTIR (Fourier transform infrared spectroscopy) spectra were confirmed on an Agilent Technologies 41630 apparatus. The elemental analysis was obtained on a Vario EL cube. PXRD (powder X-ray powder diffraction) peaks were verified using a Cu Kα radiation source on a D8 advanced Bruker-Powder-Diffractometer. The SEM (scanning electron microscopy) measurements were performed on a JSM740 Scanning Electron Microscope. A NETZSCH STA 409 PC/PG instrument was employed for recording TGA (thermogravimetric analyses) under a N_2 environment with a heating rate of 10 °C/min. Pore size and BET surface measurements were done at 77 K with N_2 sorption isotherms on the Micromeritics ASAP 2020 apparatus. Prior to the analysis, the prepared Cu-MOF effectively degassed overnight at a temperature of 150 °C as well.

■ ASSOCIATED CONTENT

Supporting Information

The Supporting Information is available free of charge at https://pubs.acs.org/doi/10.1021/acsomega.2c07137.

^{1}H NMR, C NMR, and FTIR of H_4L; PXRD and FTIR results and microscope images of Cu-MOF and PXRD before and after five cycles; ^{1}H NMR spectroscopic determination of the products; and ^{1}H NMR integration of the characteristic benzylic protons (starting, product) and conversions into products (PDF)

■ AUTHOR INFORMATION

Corresponding Authors

Adeel Hussain Chughtai − *Institute of Chemical Sciences, Bahauddin Zakariya University, Multan 60800, Pakistan;* orcid.org/0000-0002-2293-8919; Phone: +923339702072; Email: adeelhussain@bzu.edu.pk

Francis Verpoort − *Laboratory of Organometallics, Catalysis and Ordered Materials, State Key Laboratory of Advanced Technology for the Materials Synthesis and Processing, Center for the Chemical and Material Engineering, Wuhan University of Technology, Wuhan 430070, China;* orcid.org/0000-0002-5184-5500; Phone: +8618701743583; Email: francis@whut.edu.cn

Authors

Sheereen Afaq − *Institute of Chemical Sciences, Bahauddin Zakariya University, Multan 60800, Pakistan*

Muhammad Usman Akram − *Institute of Chemical Sciences, Bahauddin Zakariya University, Multan 60800, Pakistan*

https://doi.org/10.1021/acsomega.2c07137
ACS Omega 2023, 8, 6638−6649

Wasif Mahmood Ahmed Malik − *Institute of Chemical Sciences, Bahauddin Zakariya University, Multan 60800, Pakistan; Department of Chemistry, Emerson University Multan, Multan 60000, Pakistan*
Muhammad Ismail − *Institute of Chemical Sciences, Bahauddin Zakariya University, Multan 60800, Pakistan*
Abdul Ghafoor − *Institute of Chemical Sciences, Bahauddin Zakariya University, Multan 60800, Pakistan*
Muhammad Ibrahim − *Department of Biochemistry, Bahauddin Zakariya University, Multan 60800, Pakistan*
Mehr un Nisa − *Department of Chemistry, University of Lahore, Lahore 54590, Pakistan*
Muhammad Naeem Ashiq − *Institute of Chemical Sciences, Bahauddin Zakariya University, Multan 60800, Pakistan;* orcid.org/0000-0001-8561-3065

Complete contact information is available at: https://pubs.acs.org/10.1021/acsomega.2c07137

Author Contributions

The manuscript was written through equal contributions of the all authors and coauthors. All authors have approved the final form of the manuscript.

Notes

The authors declare no competing financial interest.

■ ACKNOWLEDGMENTS

The authors are very grateful to the Bahauddin Zakariya University, Multan 60800, Pakistan for providing the Research Facilities at the Institute of Chemical Sciences. The authors approvingly acknowledge State Key Laboratory of the Advanced Technology for Materials Synthesis and Processing; Center for Chemical and Material Engineering, The Wuhan University of Technology, Wuhan 430070, P.R. China, for characterization of samples.

■ REFERENCES

(1) Jenck, J. F.; Agterberg, F.; Droescher, M. J. Products and processes for a sustainable chemical industry: a review of achievements and prospects. *Green chem.* **2004**, *6* (11), 544−556.
(2) Tundo, P.; Anastas, P.; Black, D. S.; Breen, J.; Collins, T.; Memoli, S.; Miyamoto, J.; Polyakoff, M.; Tumas, W. Special topic issue on green chemistry. *Pure Appl. Chem.* **2000**, *72* (7), 1207−1228.
(3) Chakraborty, G.; Park, I.-H.; Medishetty, R.; Vittal, J. J. Two-dimensional metal-organic framework materials: Synthesis, structures, properties and applications. *Chem. Rev.* **2021**, *121* (7), 3751−3891.
(4) Fujita, M.; Kwon, Y. J.; Washizu, S.; Ogura, K. Preparation, clathration ability, and catalysis of a two-dimensional square network material composed of cadmium (II) and 4, 4′-bipyridine. *J. Am. Chem. Soc.* **1994**, *116* (3), 1151−1152.
(5) Zhang, X.; Chen, Z.; Liu, X.; Hanna, S. L.; Wang, X.; Taheri-Ledari, R.; Maleki, A.; Li, P.; Farha, O. K. A historical overview of the activation and porosity of metal−organic frameworks. *Chem. Soc. Rev.* **2020**, *49* (20), 7406−7427.
(6) Amaro-Gahete, J.; Klee, R.; Esquivel, D.; Ruiz, J. R.; Jimenez-Sanchidrian, C.; Romero-Salguero, F. J. Fast ultrasound-assisted synthesis of highly crystalline MIL-88A particles and their application as ethylene adsorbents. *Ultrason. Sonochem.* **2019**, *50*, 59−66.
(7) Hou, Q.; Zhou, S.; Wei, Y.; Caro, J.; Wang, H. Balancing the grain boundary structure and the framework flexibility through bimetallic Metal−Organic Framework (MOF) membranes for gas separation. *J. Am. Chem. Soc.* **2020**, *142* (21), 9582−9586.
(8) Wu, J.; Dai, Q.; Zhang, H.; Li, X. A defect-free MOF composite membrane prepared via in-situ binder-controlled restrained second-growth method for energy storage device. *Energy Stor. Mater.* **2021**, *35*, 687−694.
(9) Nandiyanto, A. B. D.; Okuyama, K. Progress in developing spray-drying methods for the production of controlled morphology particles: From the nanometer to submicrometer size ranges. *Adv. Powder Technol.* **2011**, *22* (1), 1−19.
(10) Liang, C.; He, J.; Zhang, Y.; Zhang, W.; Liu, C.; Ma, X.; Liu, Y.; Gu, J. MOF-derived CoNi@ C-silver nanowires/cellulose nanofiber composite papers with excellent thermal management capability for outstanding electromagnetic interference shielding. *Compos. Sci. Technol.* **2022**, *224*, 109445.
(11) Farha, O. K.; Eryazici, I.; Jeong, N. C.; Hauser, B. G.; Wilmer, C. E.; Sarjeant, A. A.; Snurr, R. Q.; Nguyen, S. T.; Yazaydın, A. O. z. r.; Hupp, J. T. Metal−organic framework materials with ultrahigh surface areas: is the sky the limit? *J. Am. Chem. Soc.* **2012**, *134* (36), 15016−15021.
(12) Furukawa, H.; Go, Y. B.; Ko, N.; Park, Y. K.; Uribe-Romo, F. J.; Kim, J.; O'Keeffe, M.; Yaghi, O. M. Isoreticular expansion of metal−organic frameworks with triangular and square building units and the lowest calculated density for porous crystals. *Inorg. Chem.* **2011**, *50* (18), 9147−9152.
(13) Bonnett, B. L.; Smith, E. D.; De La Garza, M.; Cai, M.; Haag, J. V., IV; Serrano, J. M.; Cornell, H. D.; Gibbons, B.; Martin, S. M.; Morris, A. J. PCN-222 metal−organic framework nanoparticles with tunable pore size for nanocomposite reverse osmosis membranes. *ACS Appl. Mater. Interfaces* **2020**, *12* (13), 15765−15773.
(14) Gao, D.; Chen, J.-H.; Fang, S.; Ma, T.; Qiu, X.-H.; Ma, J.-G.; Gu, Q.; Cheng, P. Simultaneous quantitative recognition of all purines including N6-methyladenine via the host-guest interactions on a Mn-MOF. *Matter.* **2021**, *4* (3), 1001−1016.
(15) Deng, H.; Grunder, S.; Cordova, K. E.; Valente, C.; Furukawa, H.; Hmadeh, M.; Gandara, F.; Whalley, A. C.; Liu, Z.; Asahina, S.; Kazumori, H.; O'Keeffe, M.; Terasaki, O.; Stoddart, J. F.; Yaghi, O. M. Large-pore apertures in a series of metal-organic frameworks. *Science.* **2012**, *336* (6084), 1018−1023.
(16) Kim, H.; Hong, C. S. MOF-74-type frameworks: Tunable pore environment and functionality through metal and ligand modification. *CrystEngComm* **2021**, *23* (6), 1377−1387.
(17) Kreno, L. E.; Leong, K.; Farha, O. K.; Allendorf, M.; Van Duyne, R. P.; Hupp, J. T. Metal−organic framework materials as chemical sensors. *Chem. Rev.* **2012**, *112* (2), 1105−1125.
(18) Bara, D.; Wilson, C.; Mörtel, M.; Khusniyarov, M. M.; Ling, S.; Slater, B.; Sproules, S.; Forgan, R. S. Kinetic Control of Interpenetration in Fe−Biphenyl-4, 4′-dicarboxylate Metal−Organic Frameworks by Coordination and Oxidation Modulation. *J. Am. Chem. Soc.* **2019**, *141* (20), 8346−8357.
(19) Liang, K.; Carbonell, C.; Styles, M. J.; Ricco, R.; Cui, J.; Richardson, J. J.; Maspoch, D.; Caruso, F.; Falcaro, P. Biomimetic replication of microscopic metal−organic framework patterns using printed protein patterns. *Adv. Mater.* **2015**, *27* (45), 7293−7298.
(20) Falahati, M.; Sharifi, M.; Ten Hagen, T. L. Explaining chemical clues of metal organic framework-nanozyme nano-/micro-motors in targeted treatment of cancers: benchmarks and challenges. *J. Nanobiotechnol.* **2022**, *20* (1), 1−26.
(21) Thorarinsdottir, A. E.; Harris, T. D. Metal−organic framework magnets. *Chem. Rev.* **2020**, *120* (16), 8716−8789.
(22) Zhao, J.-P.; Yang, Q.; Liu, Z.-Y.; Zhao, R.; Hu, B.-W.; Du, M.; Chang, Z.; Bu, X.-H. A unique substituted Co (II)-formate coordination framework exhibits weak ferromagnetic single-chain-magnet like behavior. *Chem. Commun.* **2012**, *48* (52), 6568−6570.
(23) Lama, P.; Mrozinski, J.; Bharadwaj, P. K. Co (II) coordination polymers with co-ligand dependent dinuclear to tetranuclear core: spin-canting, weak ferromagnetic, and antiferromagnetic behavior. *Cryst. Growth. Des.* **2012**, *12* (6), 3158−3168.
(24) Petit, C. Present and future of MOF research in the field of adsorption and molecular separation. *Curr. Opin. Chem. Eng.* **2018**, *20*, 132−142.
(25) Shekhah, O.; Liu, J.; Fischer, R.; Wöll, C. MOF thin films: existing and future applications. *Chem. Soc. Rev.* **2011**, *40* (2), 1081−1106.

(26) Cao, J.; Li, X.; Tian, H. Metal-organic framework (MOF)-based drug delivery. *Curr. Opin. Chem. Eng.* **2020**, *27* (35), 5949−5969.
(27) Fang, Y.; Ma, Y.; Zheng, M.; Yang, P.; Asiri, A. M.; Wang, X. Metal−organic frameworks for solar energy conversion by photoredox catalysis. *Chem. Soc. Rev.* **2018**, *373*, 83−115.
(28) Ōkawa, H.; Sadakiyo, M.; Yamada, T.; Maesato, M.; Ohba, M.; Kitagawa, H. Proton-conductive magnetic metal−organic frameworks, {NR3 (CH2COOH)}[MaIIMbIII (ox) 3]: effect of carboxyl residue upon proton conduction. *J. Am. Chem. Soc.* **2013**, *135* (6), 2256−2262.
(29) Nadeem, M.; Yasin, G.; Bhatti, M. H.; Mehmood, M.; Arif, M.; Dai, L. Pt-M bimetallic nanoparticles (M= Ni, Cu, Er) supported on metal organic framework-derived N-doped nanostructured carbon for hydrogen evolution and oxygen evolution reaction. *J. Power Sources.* **2018**, *402*, 34−42.
(30) Ahmed Malik, W. M.; Afaq, S.; Mahmood, A.; Niu, L.; Yousaf ur Rehman, M.; Ibrahim, M.; Mohyuddin, A.; Qureshi, A. M.; Ashiq, M. N.; Chughtai, A. H. A Facile Synthesis of CeO2 from GO@ Ce-MOF Precursor and Its Efficient Performance in the Oxygen Evolution Reaction. *Front. Chem.* **2022**, *10*, 1275.
(31) Ding, M.; Flaig, R. W.; Jiang, H.-L.; Yaghi, O. M. Carbon capture and conversion using metal−organic frameworks and MOF-based materials. *Chem. Soc. Rev.* **2019**, *48* (10), 2783−2828.
(32) Lustig, W. P.; Mukherjee, S.; Rudd, N. D.; Desai, A. V.; Li, J.; Ghosh, S. K. Metal−organic frameworks: functional luminescent and photonic materials for sensing applications. *Chem. Soc. Rev.* **2017**, *46* (11), 3242−3285.
(33) Allendorf, M. D.; Bauer, C. A.; Bhakta, R.; Houk, R. Luminescent metal−organic frameworks. *Chem. Soc. Rev.* **2009**, *38* (5), 1330−1352.
(34) Wu, D.; Zhang, P.-F.; Yang, G.-P.; Hou, L.; Zhang, W.-Y.; Han, Y.-F.; Liu, P.; Wang, Y.-Y. Supramolecular control of MOF pore properties for the tailored guest adsorption/separation applications. *Coord. Chem. Rev.* **2021**, *434*, 213709.
(35) Zhang, H.; Nai, J.; Yu, L.; Lou, X. W. D. Metal-organic-framework-based materials as platforms for renewable energy and environmental applications. *Joule.* **2017**, *1* (1), 77−107.
(36) Jayaramulu, K.; Mukherjee, S.; Morales, D. M.; Dubal, D. P.; Nanjundan, A. K.; Schneemann, A.; Masa, J.; Kment, S.; Schuhmann, W.; Otyepka, M.; Zboril, R.; Fischer, R. A. Graphene-Based Metal−Organic Framework Hybrids for Applications in Catalysis, Environmental, and Energy Technologies. *Chem. Rev.* **2022**, *122*, 17241.
(37) Chaemchuen, S.; Kabir, N. A.; Zhou, K.; Verpoort, F. Metal−organic frameworks for upgrading biogas via CO2 adsorption to biogas green energy. *Chem. Soc. Rev.* **2013**, *42* (24), 9304−9332.
(38) Yan, Y.; Suyetin, M.; Bichoutskaia, E.; Blake, A. J.; Allan, D. R.; Barnett, S. A.; Schröder, M. Modulating the packing of [Cu 24 (isophthalate) 24] cuboctahedra in a triazole-containing metal−organic polyhedral framework. *Chem. Sci.* **2013**, *4* (4), 1731−1736.
(39) Li, J.-R.; Sculley, J.; Zhou, H.-C. Metal−organic frameworks for separations. *Chem. Rev.* **2012**, *112* (2), 869−932.
(40) Shimizu, G. K.; Taylor, J. M.; Kim, S. Proton conduction with metal-organic frameworks. *Science.* **2013**, *341* (6144), 354−355.
(41) Chughtai, A. H.; Ahmad, N.; Younus, H. A.; Laypkov, A.; Verpoort, F. Metal−organic frameworks: versatile heterogeneous catalysts for efficient catalytic organic transformations. *Chem. Soc. Rev.* **2015**, *44* (19), 6804−6849.
(42) Jeong, K. S.; Go, Y. B.; Shin, S. M.; Lee, S. J.; Kim, J.; Yaghi, O. M.; Jeong, N. Asymmetric catalytic reactions by NbO-type chiral metal−organic frameworks. *Chem. Sci.* **2011**, *2* (5), 877−882.
(43) Lee, J.; Farha, O. K.; Roberts, J.; Scheidt, K. A.; Nguyen, S. T.; Hupp, J. T. Metal−organic framework materials as catalysts. *Chem. Soc. Rev.* **2009**, *38* (5), 1450−1459.
(44) Gascon, J.; Corma, A.; Kapteijn, F.; Llabres i Xamena, F. X. Metal organic framework catalysis: Quo vadis? *ACS Catal.* **2014**, *4* (2), 361−378.
(45) Wei, Y.-S.; Zhang, M.; Zou, R.; Xu, Q. Metal−organic framework-based catalysts with single metal sites. *Chem. Rev.* **2020**, *120* (21), 12089−12174.
(46) Yoon, M.; Srirambalaji, R.; Kim, K. Homochiral metal−organic frameworks for asymmetric heterogeneous catalysis. *Chem. Rev.* **2012**, *112* (2), 1196−1231.
(47) Zhou, Y.; Abazari, R.; Chen, J.; Tahir, M.; Kumar, A.; Ikreedeegh, R. R.; Rani, E.; Singh, H.; Kirillov, A. M. Bimetallic metal−organic frameworks and MOF-derived composites: Recent progress on electro-and photoelectrocatalytic applications. *Coord. Chem. Rev.* **2022**, *451*, 214264.
(48) Sun, C.-Y.; Qin, C.; Wang, X.-L.; Su, Z.-M. Metal-organic frameworks as potential drug delivery systems. *Expert Opin. Drug Delivery* **2013**, *10* (1), 89−101.
(49) Mahata, P.; Prabu, M.; Natarajan, S. Time-and temperature-dependent study in the three-component zinc-triazolate-oxybis (benzoate) system: Stabilization of new topologies. *Cryst. Growth. Des n* **2009**, *9* (8), 3683−3691.
(50) Milios, C. J.; Winpenny, R. E. Cluster-Based Single-Molecule Magnets. *Molecular Nanomagnets and Related Phenomena*; Springer, 2014; pp 1−109.
(51) Jensen, P.; Batten, S. R.; Fallon, G. D.; Moubaraki, B.; Murray, K. S.; Price, D. J. Structural isomers of M(dca)2 molecule-based magnets. Crystal structure of tetrahedrally coordinated sheet-like β-Zn(dca)2 and β-Co/Zn(dca)2, and the octahedrally coordinated rutile-like α-Co(dca)2, where dca− = dicyanamide, N(CN)2−, and magnetism of β-Co(dca)2. *Chem. Commun.* **1999**, 177.
(52) Lin, X.; Telepeni, I.; Blake, A. J.; Dailly, A.; Brown, C. M.; Simmons, J. M.; Zoppi, M.; Walker, G. S.; Thomas, K. M.; Mays, T. J.; Hubberstey, P.; Champness, N. R.; Schroder, M. High capacity hydrogen adsorption in Cu (II) tetracarboxylate framework materials: the role of pore size, ligand functionalization, and exposed metal sites. *J. Am. Chem. Soc.* **2009**, *131* (6), 2159−2171.
(53) Liu, J.; Chen, L.; Cui, H.; Zhang, J.; Zhang, L.; Su, C.-Y. Applications of metal−organic frameworks in heterogeneous supramolecular catalysis. *Chem. Soc. Rev.* **2014**, *43* (16), 6011−6061.
(54) Custelcean, R.; Gorbunova, M. G. A metal-organic framework functionalized with free carboxylic acid sites and its selective binding of a Cl (H_2O) 4-cluster. *J. Am. Chem. Soc.* **2005**, *127* (47), 16362−16363.
(55) Shin, D. M.; Lee, I. S.; Chung, Y. K. Self-assemblies of new rigid angular ligands and metal centers toward the rational construction and modification of novel coordination polymer networks. *Inorg. Chem.* **2003**, *42* (26), 8838−8846.
(56) Hou, X.-J.; He, P.; Li, H.; Wang, X. Understanding the Adsorption Mechanism of C_2H_2, CO_2, and CH_4 in Isostructural Metal−Organic Frameworks with Coordinatively Unsaturated Metal Sites. *J. Phys. Chem. C* **2013**, *117* (6), 2824−2834.
(57) Opanasenko, M.; Dhakshinamoorthy, A.; Čejka, J.; Garcia, H. Deactivation pathways of the catalytic activity of metal−organic frameworks in condensation reactions. *ChemCatChem.* **2013**, *5* (6), 1553−1561.
(58) Chen, B.; Wang, L.; Xiao, Y.; Fronczek, F. R.; Xue, M.; Cui, Y.; Qian, G. A luminescent metal−organic framework with Lewis basic pyridyl sites for the sensing of metal ions. *Angew. Chem., Int. Ed.* **2009**, *48* (3), 500−503.
(59) Garibay, S. J.; Cohen, S. M. Isoreticular synthesis and modification of frameworks with the UiO-66 topology. *Chem. Commun.* **2010**, *46* (41), 7700−7702.
(60) Gascon, J.; Aktay, U.; Hernandez-Alonso, M. D.; van Klink, G. P.; Kapteijn, F. Amino-based metal-organic frameworks as stable, highly active basic catalysts. *J. Catal.* **2009**, *261* (1), 75−87.
(61) Lin, X.-M.; Li, T.-T.; Chen, L.-F.; Zhang, L.; Su, C.-Y. Two ligand-functionalized Pb (II) metal−organic frameworks: structures and catalytic performances. *Dalton Trans.* **2012**, *41* (34), 10422−10429.
(62) Knoevenagel, E. Condensation von Malonsäure mit aromatischen Aldehyden durch Ammoniak und Amine. *Ber. Dtsch. Chem. Ges.* **1898**, *31* (3), 2596−2619.
(63) Freeman, F. Properties and reactions of ylidenemalononitriles. *Chem. Rev.* **1980**, *80* (4), 329−350.

https://doi.org/10.1021/acsomega.2c07137
ACS Omega 2023, 8, 6638−6649

(64) Volkova, M. S.; Jensen, K. C.; Lozinskaya, N. A.; Sosonyuk, S. E.; Proskurnina, M. V.; Mesecar, A. D.; Zefirov, N. S. Synthesis of novel MT3 receptor ligands via an unusual Knoevenagel condensation. *Bioorg. Med. Chem. Lett.* **2012**, *22* (24), 7578−7581.
(65) Moghaddam, F. M.; Mirjafary, Z.; Javan, M. J.; Motamen, S.; Saeidian, H. Facile synthesis of highly substituted 2-pyrone derivatives via a tandem Knoevenagel condensation/lactonization reaction of β-formyl-esters and 1, 3-cyclohexadiones. *Tetrahedron lett.* **2014**, *55* (18), 2908−2911.
(66) Beutler, U.; Fuenfschilling, P. C.; Steinkemper, A. An improved manufacturing process for the antimalaria drug coartem. Part II. *Org. Process Res. Dev.* **2007**, *11* (3), 341−345.
(67) Toovey, S.; Jamieson, A.; Nettleton, G. Successful co-artemether (artemether−lumefantrine) clearance of falciparum malaria in a patient with severe cholera in Mozambique. *Travel Med. Infect. Dis.* **2003**, *1* (3), 177−179.
(68) Keating, G.; O'Kennedy, R. The chemistry and occurrence of coumarins. *Coumarins: Biology, Applications and Mode of Action*; John Wiley & Sons, Inc.: New York, 1997; Vol *348*.
(69) Barnes, D. M.; Haight, A. R.; Hameury, T.; McLaughlin, M. A.; Mei, J.; Tedrow, J. S.; Riva Toma, J. D. New conditions for the synthesis of thiophenes via the Knoevenagel/Gewald reaction sequence. Application to the synthesis of a multitargeted kinase inhibitor. *Tetrahedron* **2006**, *62* (49), 11311−11319.
(70) Lyall, R.; Zilberstein, A.; Gazit, A.; Gilon, C.; Levitzki, A.; Schlessinger, J. Tyrphostins inhibit epidermal growth factor (EGF)-receptor tyrosine kinase activity in living cells and EGF-stimulated cell proliferation. *J. Biol. Chem.* **1989**, *264* (24), 14503−14509.
(71) Opanasenko, M.; Dhakshinamoorthy, A.; Shamzhy, M.; Nachtigall, P.; Horáček, M.; Garcia, H.; Čejka, J. Comparison of the catalytic activity of MOFs and zeolites in Knoevenagel condensation. *Catal. Sci. Technol.* **2013**, *3* (2), 500−507.
(72) Le, W.-J.; Lu, H.-F.; Zhou, J.-T.; Cheng, H.-L.; Gao, Y.-H. Synthesis of a new urea derivative: a dual-functional organocatalyst for Knoevenagel condensation in water. *Tetrahedron lett.* **2013**, *54* (39), 5370−5373.
(73) Shrikhande, J. J.; Gawande, M. B.; Jayaram, R. V. Cross-aldol and Knoevenagel condensation reactions in aqueous micellar media. *Catal. Commun.* **2008**, *9* (6), 1010−1016.
(74) Zhu, A.; Liu, R.; Li, L.; Li, L.; Wang, L.; Wang, J. Dual functions of N, N-dimethylethanolamnium-based ionic liquids for the Knoevenagel reactions at room temperature. *Catal. Today* **2013**, *200*, 17−23.
(75) Zhao, J.; Xie, J.; Au, C.-T.; Yin, S.-F. One-pot synthesis of potassium-loaded MgAl oxide as solid superbase catalyst for Knoevenagel condensation. *Appl. Catal. A: Gen.* **2013**, *467*, 33−37.
(76) Saravanamurugan, S.; Palanichamy, M.; Hartmann, M.; Murugesan, V. Knoevenagel condensation over β and Y zeolites in liquid phase under solvent free conditions. *Appl. Catal. A: Gen.* **2006**, *298*, 8−15.
(77) Kantevari, S.; Bantu, R.; Nagarapu, L. HClO4−SiO2 and PPA−SiO_2 catalyzed efficient one-pot Knoevenagel condensation, Michael addition and cyclo-dehydration of dimedone and aldehydes in acetonitrile, aqueous and solvent free conditions: Scope and limitations. *J. Mol. Catal. A: Chem.* **2007**, *269* (1), 53−57.
(78) Cheng, R.-R.; Shao, S.-X.; Wu, H.-H.; Niu, Y.-F.; Han, J.; Zhao, X.-L. A dual functional porous NbO-type metal−organic framework decorated with acylamide groups for selective sorption and catalysis. *Inorg. Chem. Commun.* **2014**, *46* (0), 226−228.
(79) Duan, J.; Higuchi, M.; Foo, M. L.; Horike, S.; Rao, K. P.; Kitagawa, S. A family of rare earth porous coordination polymers with different flexibility for CO_2/C_2H_4 and CO_2/C_2H_6 separation. *Inorg. Chem.* **2013**, *52* (14), 8244−8249.
(80) Kostakis, G. E.; Casella, L.; Boudalis, A. K.; Monzani, E.; Plakatouras, J. C. Structural variation from 1D chains to 3D networks: a systematic study of coordination number effect on the construction of coordination polymers using the terepthaloylbisglycinate ligand. *New J. Chem.* **2011**, *35* (5), 1060−1071.
(81) Zheng, B.; Bai, J.; Duan, J.; Wojtas, L.; Zaworotko, M. J. Enhanced CO_2 binding affinity of a high-uptake rht-type metal−organic framework decorated with acylamide groups. *J. Am. Chem. Soc.* **2011**, *133* (4), 748−751.
(82) Duan, J.; Yang, Z.; Bai, J.; Zheng, B.; Li, Y.; Li, S. Highly selective CO_2 capture of an agw-type metal−organic framework with inserted amides: experimental and theoretical studies. *Chem. Commun.* **2012**, *48* (25), 3058−3060.
(83) Hua, J.-A.; Zhao, Y.; Liu, Q.; Zhao, D.; Chen, K.; Sun, W.-Y. Zinc (ii) coordination polymers with substituted benzenedicarboxylate and tripodal imidazole ligands: syntheses, structures and properties. *CrystEngComm* **2014**, *16* (32), 7536−7546.
(84) Zou, Y.; Yu, C.; Li, Y.; Lah, M. S. A 3-dimensional coordination polymer with a rare lonsdaleite topology constructed from a tetrahedral ligand. *CrystEngComm* **2012**, *14* (21), 7174−7177.
(85) Zheng, B.; Liu, H.; Wang, Z.; Yu, X.; Yi, P.; Bai, J. Porous NbO-type metal−organic framework with inserted acylamide groups exhibiting highly selective CO_2 capture. *CrystEngComm* **2013**, *15* (18), 3517−3520.
(86) Wu, C.-D.; Hu, A.; Zhang, L.; Lin, W. A homochiral porous metal-organic framework for highly enantioselective heterogeneous asymmetric catalysis. *J. Am. Chem. Soc.* **2005**, *127* (25), 8940−8941.
(87) Gomez-Lor, B.; Gutierrez-Puebla, E.; Iglesias, M.; Monge, M.; Ruiz-Valero, C.; Snejko, N. Novel 2D and 3D indium metal-organic frameworks: Topology and catalytic properties. *Chem. Mater.* **2005**, *17* (10), 2568−2573.
(88) Cho, S.-H.; Ma, B.; Nguyen, S. T.; Hupp, J. T.; Albrecht-Schmitt, T. E. A metal−organic framework material that functions as an enantioselective catalyst for olefin epoxidation. *Chem. Commun.* **2006**, *24*, 2563−2565.
(89) Vimont, A.; Goupil, J.-M.; Lavalley, J.-C.; Daturi, M.; Surblé, S.; Serre, C.; Millange, F.; Férey, G.; Audebrand, N. Investigation of acid sites in a zeotypic giant pores chromium (III) carboxylate. *J. Am. Chem. Soc.* **2006**, *128* (10), 3218−3227.
(90) Seo, J. S.; Whang, D.; Lee, H.; Jun, S. I.; Oh, J.; Jeon, Y. J.; Kim, K. A homochiral metal−organic porous material for enantioselective separation and catalysis. *Nature.* **2000**, *404* (6781), 982−986.
(91) Uemura, T.; Kitaura, R.; Ohta, Y.; Nagaoka, M.; Kitagawa, S. Nanochannel-Promoted Polymerization of Substituted Acetylenes in Porous Coordination Polymers. *Angew. Chem., Int. Ed.* **2006**, *118* (25), 4218−4222.
(92) Shin, D. M.; Lee, I. S.; Chung, Y. K. Rational synthesis and characterization of robust microporous metal-organic frameworks with base functionality. *Cryst. Growth Des.* **2006**, *6* (5), 1059−1061.
(93) Huang, G.-Q.; Chen, J.; Huang, Y.-L.; Wu, K.; Luo, D.; Jin, J.-K.; Zheng, J.; Xu, S.-H.; Lu, W. Mixed-Linker Isoreticular Zn (II) Metal−Organic Frameworks as Brønsted Acid−Base Bifunctional Catalysts for Knoevenagel Condensation Reactions. *Inorg. Chem.* **2022**, *61*, 8339.
(94) Hasegawa, S.; Horike, S.; Matsuda, R.; Furukawa, S.; Mochizuki, K.; Kinoshita, Y.; Kitagawa, S. Three-dimensional porous coordination polymer functionalized with amide groups based on tridentate ligand: selective sorption and catalysis. *J. Am. Chem. Soc.* **2007**, *129* (9), 2607−2614.
(95) Li, G.-W.; Xiao, J.; Zhang, W.-Q. Highly efficient Knoevenagel condensation reactions catalyzed by a proline-functionalized polyacrylonitrile fiber. *Chin. Chem. Lett.* **2013**, *24* (1), 52−54.
(96) Shanthan Rao, P.; Venkataratnam, R.V. Zinc chloride as a new catalyst for Knoevenagel condensation. *Tetrahedron lett.* **1991**, *32* (41), 5821−5822.
(97) Liu, Q.; Ai, H.-M. Sodium benzoate as a green, efficient, and recyclable catalyst for knoevenagel condensation. *Synth. commun.* **2012**, *42* (20), 3004−3010.
(98) Narsaiah, A. V.; Nagaiah, K. An efficient knoevenagel condensation catalyzed by LaCl3. 7H2O in heterogeneous medium. *Synth. commun.* **2003**, *33* (21), 3825−3832.
(99) Gandhi, S.; Sharma, V.; Koul, I. S.; Mandal, S. K. Shedding Light on the Lewis Acid Catalysis in Organic Transformations Using a Zn-MOF Microflower and Its ZnO Nanorod. *Catal. Lett.* **2022**, 1−16.

https://doi.org/10.1021/acsomega.2c07137
ACS Omega 2023, 8, 6638−6649

(100) Tom, L.; Kurup, M. A 2D-layered Cd (II) MOF as an efficient heterogeneous catalyst for the Knoevenagel reaction. *J. Solid State Chem.* **2021**, *294*, 121846.
(101) Parmar, B.; Patel, P.; Murali, V.; Rachuri, Y.; Kureshy, R. I.; Khan, N.-u. H.; Suresh, E. Efficient heterogeneous catalysis by dual ligand Zn (II)/Cd (II) MOFs for the Knoevenagel condensation reaction: adaptable synthetic routes, characterization, crystal structures and luminescence studies. *Inorg. Chem. Front.* **2018**, *5* (10), 2630−2640.
(102) Chen, H.; Zhang, T.; Liu, S.; Lv, H.; Fan, L.; Zhang, X. Fluorine-functionalized NbO-type $\{Cu_2\}$-organic framework: enhanced catalytic performance on the cycloaddition reaction of CO_2 with epoxides and deacetalization-knoevenagel condensation. *Inorg. Chem.* **2022**, *61* (30), 11949−11958.
(103) Hu, D.; Kluger, R. Functional Cross-Linked Hemoglobin Bistetramers: Geometry and Cooperativity. *Biochemistry.* **2008**, *47* (47), 12551−12561.

https://doi.org/10.1021/acsomega.2c07137
ACS Omega 2023, 8, 6638−6649